ARTICLE

Active and Optically Transparent Tetracationic Porphyrin/TiO_2 Composite Thin Films

Pedro Castillero,[†,‡] Juan R. Sánchez-Valencia,[‡] Manuel Cano,[†] José M. Pedrosa,[*,†] Javier Roales,[†] Angel Barranco,[‡] and Agustín R. González-Elipe[‡]

Departamento de Sistemas Físicos, Químicos y Naturales, Universidad Pablo de Olavide, Carretera Utrera km 1, E-41013 Sevilla, Spain, and Instituto de Ciencia de Materiales de Sevilla, Universidad de Sevilla-CSIC, Américo Vespucio 49, E-41092, Sevilla, Spain

ABSTRACT Fluorescent tetracationic porphyrin (TMPyP) molecules have been incorporated into optically transparent TiO_2 thin films acting as a host material. The films, with a columnar structure and open pores, were prepared by electron evaporation at glancing angles (GAPVD). The open porosity of the films has been estimated by measuring a water adsorption isotherm with a quartz crystal monitor. TMPyP molecules were infiltrated in the host thin films by their immersion into water solutions at controlled values of pH. The state of the adsorbed molecules, the infiltration efficiency, and the adsorption kinetics were assessed by analyzing the optical response of the films by UV−vis absorption and fluorescence techniques. The infiltration efficiency was directly correlated with the acidity of the medium, increasing at basic pHs as expected from simple considerations based on the concepts of the point of zero charge (PZC) developed for colloidal oxides. By a quantitative evaluation based on the analysis of the UV spectra, the infiltration process has been described by a Langmuir type adsorption isotherm and an Elovich-like kinetics. The accessibility of the infiltrated molecules in the TMPyP/TiO_2 composite films is assessed by following the changes of their optical properties when exposed to the acid vapors and their subsequent recovery with time.

KEYWORDS: infiltration • TMPyP • TiO_2 • GAPVD • optically active composites • porous thin films.

INTRODUCTION

Porphyrin (phy) compounds have been extensively used as active components for molecular devices such as molecular photodiodes, solar cells, and optical sensors (1−5). Devices based on these compounds are gaining interest because of their outstanding optical and electrical properties and because of their low cost as compared with inorganic semiconductors. In particular, the direct use of this family of molecules for gas detection purposes has been recently highlighted by Rakow et al. (6) who have shown that they can be used for detecting a large variety of organic products with high selectivity and sensitivity.

Porphyrins with four positively charged pyridinium groups are interesting dyes because of their relatively low reduction potential (7), and high affinity for negatively charged solid surfaces (8). Although in the solid state the porphyrin redox potentials maybe somewhat different from those in solution (9, 10), these two properties make these compounds suitable for the synthesis of a large variety of composite materials incorporating these molecules (e.g., as sensitizers for wide gap semiconductors, sensor devices, etc.). Fluorescent porphyrins have also been grown as monolayers films for sensing applications (11), although the design of solid-sate sensor platforms using fluorescence detection is still a challenge. In the present investigation, we have selected the fourth charged porphyrin because its incorporation into the open microstructure of TiO_2 thin films may be favored by controlling the surface charge on this oxide host by simply adjusting the pH of the medium. This approach has been previously used by us to incorporate Rhodamine molecules into this type of thin films (12, 13).

A considerable number of papers have dealt in the literature with the optical properties of the porphyrins and their incorporation into the pores of a large variety of materials, mainly in powder form (14−18). An innovative aspect of the present work is the fact that the dye molecules are incorporated into thin films of a transparent oxide, an approach that to our knowledge has not been addressed previously in the literature. In particular, we study the incorporation of porphyrin molecules within a new type of nondispersive thin films of TiO_2 formed by a columnar microstructure with wide open voids. With respect to other dispersive solids in powder form infiltrated with dyes, the dye molecules in solution, or as monolayer films (11), we have shown that the preparation of optically transparent composite thin films provides a way for the integration of the functional optically based properties of the porphyrin molecules into photonic structures for its direct monitoring in final fluorescence sensor devices.

The TiO_2 films used as hosts have been prepared by glancing angle physical vapor deposition (GAPVD), a technique known to yield very open and porous microstructures

* To whom correspondence should be addressed. E-mail: jmpedpoy@upo.es.
Received for review October 30, 2009 and accepted January 18, 2010
† Universidad Pablo de Olavide.
‡ Universidad de Sevilla-CSIC.
DOI: 10.1021/am900746q

Published on Web 02/10/2010

formed by columns and, if controlled, other geometrical forms (19−23). This method is a modification of the electron evaporator procedure used by the ophthalmic industry to cover lenses with dense optical coatings. Here the pore structure of the prepared films has been characterized by measuring water adsorption isotherms with a quartz crystal monitor, one of the few procedures available to directly measure the porosity in thin films (24).

Because of the quite open and porous microstructure of the GAPVD thin films, they seem ideal for the development of photonic devices by incorporating optically active molecules or compounds. On the basis of these features, we propose here a new simple procedure for the incorporation of a tetracationic porphyrin (TMPyP) into this type of thin films and study their optical behavior as a function of the variables of the process. Within this context, we first present a phenomenological study of the adsorption equilibrium and kinetic control of the infiltration process. Second, we investigate the optical and spectroscopic properties of the TMPyP/TiO_2 composite thin films with the purpose of ascertaining the state of the molecule and the fluorescence efficiency of the films. Finally, the accessibility of the TMPyP/TiO_2 films to gaseous compounds from the environment and the possibility of following the optical changes of the films are checked by their exposure to acid vapors from a HCl solution. The fact that both the UV−vis and fluorescence spectra of the TMPyP/TiO_2 films are reversibly modified sustains that the high porosity of the composites ensures the accessibility of the infiltrated molecules to gaseous compounds from the environment and the reversibility of this process, two conditions that are necessary (although not sufficient) for the preparation of optical sensors.

MATERIALS AND METHODS

Preparation of TiO_2 Thin Films. TMPyP/TiO_2 composites were prepared by using porous TiO_2 thin films as host materials. For this purpose, transparent and amorphous films were prepared by GAPVD at room temperature on quartz and silicon substrates. The glancing geometry produces films with a tilted columnar microstructure (19, 23). A characteristic of these films is that they are very porous and, therefore, are characterized by relatively low refractive index values. For the present work the substrates were placed at an angle of 70° with respect to the evaporator source. The films had a thickness of approximately 350 nm.

TiO_2 Thin Film Characterization. The microstructure of the TiO_2 thin films deposited on a silicon wafer was examined by field emission scanning electron microscopy (FESEM) in a Hitachi S5200 microscope. Cross-sectional views were obtained by cleaving the silicon substrates.

Refractive indices (n) were determined by UV−vis Absorption Spectroscopy. A detailed description of these experiments can be found in previous works (25) and additional data are gathered in the Supporting Information, Figure S1.

Because of the extraordinary small amount of material available in the prepared TiO_2 thin films, determination of porosity of this kind of materials is not straightforward by the classical BET methods based on the adsorption of gases (N_2, Kr, etc.) at their condensation temperature (26). The commercial apparatus intended for this purpose uses glass containers which are not easily adaptable to thin films deposited on a rigid substrate, facing in addition the problem of the small amount of porous material available for the measurement. To overcome this problem, we have developed a new method based on the use of a quartz crystal monitor (QCM) and the measurement of water adsorption isotherms at room temperature (24). A full account of the experimental method and the procedure used to extract pore size distributions can be found in this previous paper.

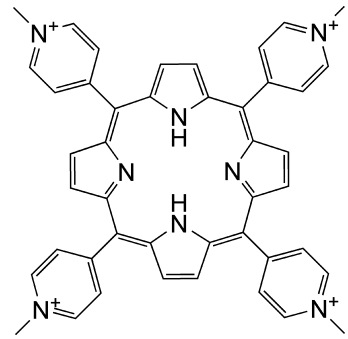

FIGURE 1. Schematic representation of the structure of the TMPyP molecular ion.

Infiltration of Dye Molecules into TiO_2 Porous Films. 5,10,15,20-Tetrakis(1-methyl-4-pyridyl)-21H,23H-porphyrin (TMPyP, Aldrich) was used without further purification. Unless otherwise stated, a 1×10^{-5} M solution of the dye in water at controlled values of pH was used for these experiments. All other reagents were Merck a.g. and used as supplied. Ultrapure water from a Millipore Milli-Q-Plus system was used throughout. A scheme of the structure of the TMPyP molecule is presented in Figure 1.

The pH of the solution was controlled between 1.9 and 10.9 by adding defined amounts of HCl or NaOH. The TiO_2 films were immersed in one of these solutions and maintained there for 1 h, except for the kinetics study. Afterward, the samples were taken out from the solution and washed with water at the same pH. With this washing, any dye molecule that is not incorporated into the thin films is removed from their surface. The films were then dried in a two step process: first by blowing nitrogen onto their surfaces for 5 mins and then by a heating at 110 °C during 1 h. After these treatments, the composite thin films presented the characteristic yellowish color of porphyrin thin films. The intensity of the color changed with the pH of the solution, a feature that pointed out that the dye adsorption degree is dependent on this parameter.

Determination of Optical Properties of the TMPyP/TiO_2 Composite Thin Films. UV−visible spectra of the composites (TMPyP/TiO_2) films were recorded on a Cary 100 Conc UV−visible spectrophotometer. Spectra are presented in absorbance after subtracting a spectrum of the TiO_2 substrate. This is an important step of the data treatment protocol to remove the interference oscillations characteristic of a thin film with a higher refraction index than the substrate (see the Supporting Information, Figure S1). In our case, this procedure is necessary to evidence some small features of the spectra of the TMPyP molecules (i.e., the so-called Q bands, see the next section). Spectra of the films were also measured with polarized light (s and p) at 0, 30, 45, 60, and 90° of incidence angle. All the experiments were carried out at least four times.

Fluorescence spectra of the composite TMPyP/TiO_2 films were recorded in a Jobin-Yvon Fluorolog3 spectrofluorometer using grids of 2 nm for the excitation and 4 nm for emission. Depending on the samples, the fluorescence spectra were excited with radiation of 430 nm and recorded in the front-face configuration.

The amount of dye molecules incorporated into the films was assessed after desorption from the film by its prolonged stirring in a 3 M KCl aqueous solution until total film discoloration. This

procedure leads to the replacement of the porphyrin molecules incorporated into the TiO_2 host thin film by K^+ ions. The dye solutions resulting from this stirring were measured by optical absorption spectroscopy and the absorption intensity compared with the data of a calibration curve obtained from different reference solutions of the dye.

The amount of TMPyP incorporated into the films was expressed as an equivalent surface concentration of porphyrin (Γ). This Γ was calculated as

$$\Gamma = \frac{(\mathrm{Abs}/\varepsilon l)V_{\mathrm{sol}}}{\mathrm{Area}_{\mathrm{film}}} \quad (1)$$

Where Abs is the absorbance of the solution measured after desorption (in the maxima of Soret band at 423 nm (27), ε the extinction coefficient of the dye, l the optical pass length, V_{Sol} the volume of the 3 M KCl aqueous solution used to the desorption and $\mathrm{Area}_{\mathrm{film}}$ the area of the film employed.

A more straightforward way to ascertain the amount of infiltrated TMPyP molecules is the use of the Lambert−Beer law for two-dimensional systems (28). Using this method, the surface concentration Γ can be calculated by

$$\Gamma = \frac{\int_{\mathrm{band}} \mathrm{Abs}_{\mathrm{film}} d\lambda}{10^3 \int_{\mathrm{band}} \varepsilon d\lambda} \quad (2)$$

Where $\mathrm{Abs}_{\mathrm{film}}$ is the absorbance directly measured in the composite film. In eq 2, we compare the area under the Soret band in the spectra for the composite films with that in solution. This is due to the spectral alterations (peak shifting and broadening) observed in our films that are usually induced by molecular association and/or conformation changes in the infiltrated TMPyP molecules (28−30). Details on the validity of this method can be found in the Supporting Information, S2. It should be noted that the use of this method allow a more direct estimation of Γ avoiding the desorption procedure. The surface concentration data reported in this paper have been estimated according to eq 2 and using the desorption method as a reference.

RESULTS AND DISCUSSION

TiO_2 Thin Film Microstructure. Figure 2 shows FESEM normal and cross-section images corresponding to TiO_2 thin films prepared by GAPVD at an angle of 70° with respect to the evaporation source. The angle formed by the columns and the substrate for the 70° as evaporation angle was approximately of 60°, as shown in the image. Films of this kind have been used as host material for the different adsorption/desorption experiments discussed in the next sections. The TiO_2 thin films are highly porous as deduced from the FESEM micrographs in Figure 2 and from the value of their refraction index, estimated as 1.79 (see the Supporting Information, Figure S1). This value is much smaller than that corresponding to the bulk material (i.e., 2.49 for TiO_2 in the form of anatase) and is a clear proof of the high porosity of the film, as previously shown for other similar nanostructures (31). A closer inspection of Figure 2 reveals that the observed void apertures are in the form of mesopores (i.e., pores larger than 2 nm) extending from the surface up to the bottom of the film. In principle, this should

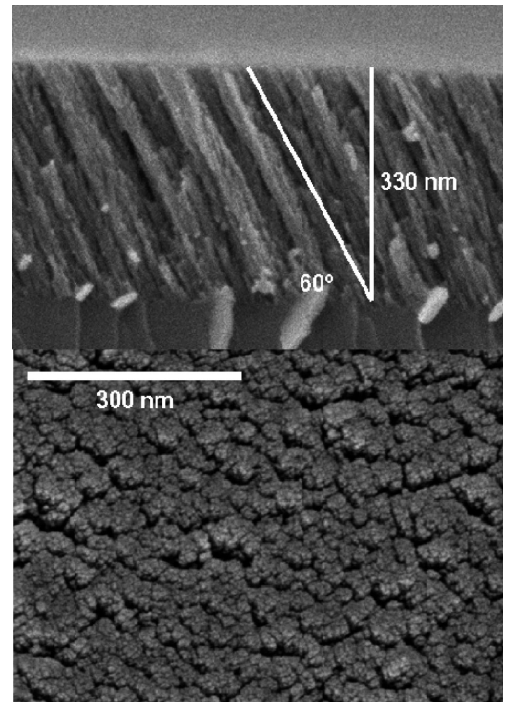

FIGURE 2. Cross-section and planar views of the TiO_2 thin films used as host of TMPyP molecules.

facilitate the accessibility of large molecules like porphyrins during the composite preparation and improves subsequent applications that would require a fast diffusion of target molecules through the film structure.

For a proper characterization of the films, it is important to have a direct assessment of the porosity of the films. Figure 3 (top) shows the water adsorption/desorption isotherms measured with a QCM according to the procedure described in ref 24. It is worth noting in this plot that some water incorporated in the pores of the films during the first adsorption cycle remained irreversibly adsorbed after desorption. This water is mainly filling micropores and its removal requires to heat the film at moderate temperatures (i.e., $t > 110$ °C). This result suggests that the pores of the TMPyP/TiO_2 composite films must be partially filled with condensed water from the atmosphere and/or residual water from the solutions where the immersion experiments were carried out. Drying either by flowing nitrogen onto the surface of the films or by heating the films at 110 °C must contribute to removal of this water.

From the analysis of these isotherms, it is also possible to extract the corresponding pore size distribution curves (24). Figure 3 (bottom) shows the corresponding curves in the range $2r > 2$ nm where the Kelvin equation for capillary condensation is applicable. From them, it is possible to conclude that in these GAPVD thin films there is a continuous variation in the pore sizes in the whole range from micropores (pores diameter < 2 nm) to mesopores (pore diameter > 2 nm). An evaluation based on the t-plot methodology (32) yields as a result that 30% of pores consist of micropores. The pore size distribution curves also indicate the existence of mesopores with pore diameters comprised between 2 and 6 nm. Pores as large as 14 nm are also

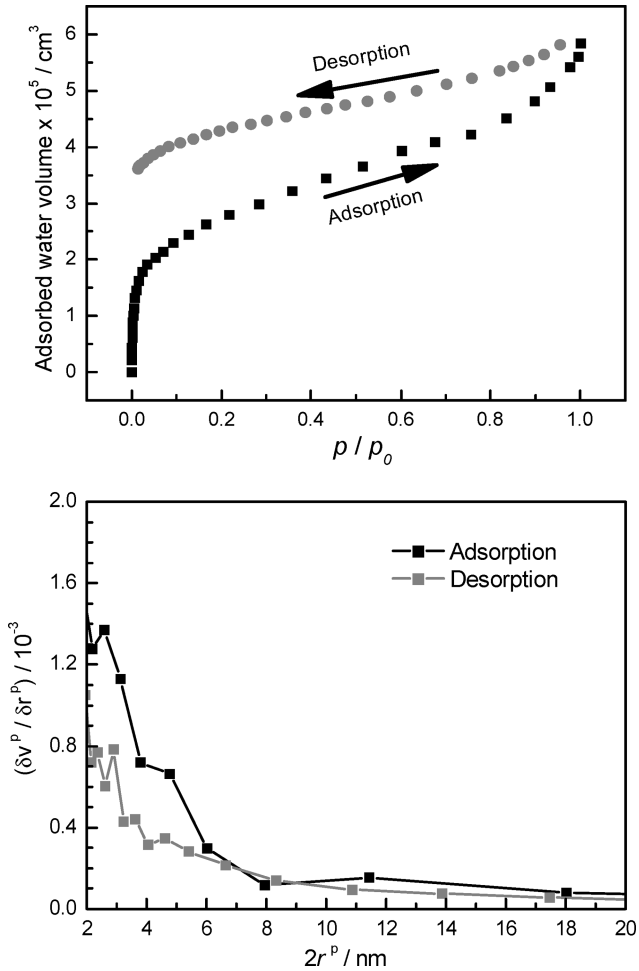

FIGURE 3. (Top) Water adsorption and desorption isotherms of the films measured with a QCM. (Bottom) Pore size distribution curves derived from the adsorption isotherms.

present in the film. After evaluation of the total water adsorption, a total pore volume of 49% can be estimated for these films.

UV−Vis Absorption Spectra of TMPyP/TiO_2 Composite Thin Films. Effective infiltration of the dye into the columnar microstructure of the films is achieved by controlling the pH of the solution. This can be directly deduced from Figure 4 showing the spectrum of TMPyP in water solution and of this molecule incorporated into the columnar film by infiltration at pH 6.9 and subsequent drying, first by blowing nitrogen and then by heating at 110 °C. Similar results were obtained for other pHs. All the spectra exhibit the typical strong Soret band of this molecule located in the region 400−450 nm along with the four weak Q bands in the range 500−650 nm (27). However, the maximum absorption of the TMPyP infiltrated into the transparent TiO_2 thin films is 14 nm red-shifted and broadened with respect to the water solution spectrum whose maximum appears at 423 nm. This last value for the wavelength of the *Soret* band in water solution coincides with that found by other authors (27, 33, 34). According to Figure 4, the overall shift in the position of the Soret band in the TMPyP/TiO_2 composites occurs in two stages, following the two successive drying steps of the preparation

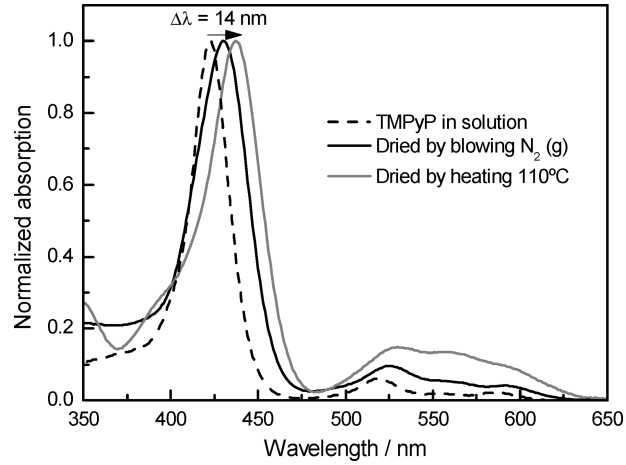

FIGURE 4. UV−visible absorption spectra recorded for the TMPyP in aqueous solution and in the composite TMPyP/TiO_2 thin films at the different steps of the preparation protocol.

protocol. First, after blowing nitrogen onto the sample, there is a shift of around 7 nm with respect to the position of the band for the TMPyP in water solution. A second shift by 7 nm then takes place after the samples are heated at 110 °C.

The shifting and broadening of the Soret band is a usual phenomenon when porphyrins are incorporated into solids or, under specific conditions, in solution. In particular, a red shift has been observed for TMPyP when adsorbed in a number of host materials. This shift has been related with different physical and/or chemical changes in the porphyrin molecular structure. Thus, Chernia et al. (29) proposed a flattening of the porphyrin molecule (through its charged peripheral methylpyridyl groups) to explain red shifts of 30 and 60 nm for the dye the adsorption and intercalation, respectively, in the clay mineral Laponite. Also, protonation of the porphyrin ring (imino nitrogens) has been suggested for soda-lime glass coated with TMPyP-doped silica sol−gels (35). In this case the Soret band shifted from 423 to 435 nm, although the main changes affected the Q-band region where the original four bands turned into two bands due to the higher molecular symmetry (D_{4h}) and the degeneration of the excited state of the protonated porphyrin. In our case, no changes in the number of Q bands are observed, suggesting the absence of significant structural modifications in the infiltrated porphyrins that should maintain their original D_{2h} molecular symmetry.

Another possible explanation for spectral red shift of TMPyP is the formation of J-aggregates (e.g., dimers) through an appropriate compensation of the peripheral positive charges to avoid repulsion. This intermolecular interaction between the porphyrin rings has been proposed for TMPyP in aqueous solution through ion-pair interactions with four BH_4^- anions (34). Further structural details have been given for Langmuir−Blodgett (LB) films of TMPyP attached to a carboxylic calixarene matrix where a compensation of charges between the two components has been demonstrated (28). We think that the initial shift of 7 nm with respect to the water solution can be attributed to a change in the environment of monomeric porphyrin molecules due to their anchoring onto the surface of TiO_2. The additional

shift to 437 nm, found after heating at 110 °C, coincides with the elimination of the hydration water condensed in the pores (see the adsorption isotherm in Figure 3), and points to additional changes in the molecular/electronic structure related with the hydration state of the molecules. Further discussion on this point will be presented below in section 6 dealing with the fluorescence behavior of the films.

Because of the tilted microstructure of the columnar TiO_2 thin films, it might happen that the adsorbed dye molecules exhibit a preferred orientation along the tilting angle of the columns. To clarify this point, we have analyzed the samples by using UV−vis with s and p polarized light for different angles of incidence. The result of this analysis shows almost coincident spectra in all cases, indicating that the porphyrin molecules are randomly oriented in the film (see the Supporting Information, Figure S3).

pH Dependence and TMPyP Infiltration Capacity. The amount of TMPyP molecules that can be infiltrated into the columnar TiO_2 thin film was dependent on the pH, the immersion time, and the porphyrin concentration in the solution employed to carry out the infiltration experiments. In this section, we will discuss the effect of pH in the infiltration efficiency. Figure 5 (top) shows a series of UV−vis absorption spectra recorded for thin films with a similar thickness immersed for one hour in a 1×10^{-5} M water solution of TMPyP at increasing pHs. Figure 5 (middle) shows an image taken for the composite thin films prepared at the indicated pHs and a 4×10^{-5} M water solution of this dye molecule. It is important to note that the cuvette used to keep the dye solution had a thickness of 1 mm and that the total number of molecules in the optical path was within the same order of magnitude that the number of molecules incorporated into the composite film prepared at pH 9.6. From the evolution of the intensities of these spectra, it is apparent that the adsorption efficiency is directly correlated with the acidity of the medium, increasing with the pH. Another feature that can be observed in Figure 5 (top) is the very similar shape of all spectra, indicating that there is no significant change in the adsorption and/or aggregation state of the TMPyP molecules when their amount into the film increases as an effect of the pH.

A quantitative assessment of the pH dependence of the amount of TMPyP molecules incorporated into the TiO_2 films is depicted in the Figure 5 (bottom), where the absorption intensity in the maxima of the Soret band and the surface concentration of dye molecules are plotted against the pH of the solution. The curves show that almost no infiltration occurs at pHs lower that 3.5. Some infiltration takes place in the range 3.5−5.5, whereas a sharp infiltration onset starts at pH 4.9 to reach a maximum at a pH of 10. From this value on, a slight decrease in the infiltration capacity is observed.

A similar tendency has been previously reported by us for Rhodamine-6G dye molecules incorporated into columnar TiO_2 thin films (12). This behavior was explained with simple considerations based on the concepts of the point of zero charge (PZC) in colloidal oxides (36, 37). According to

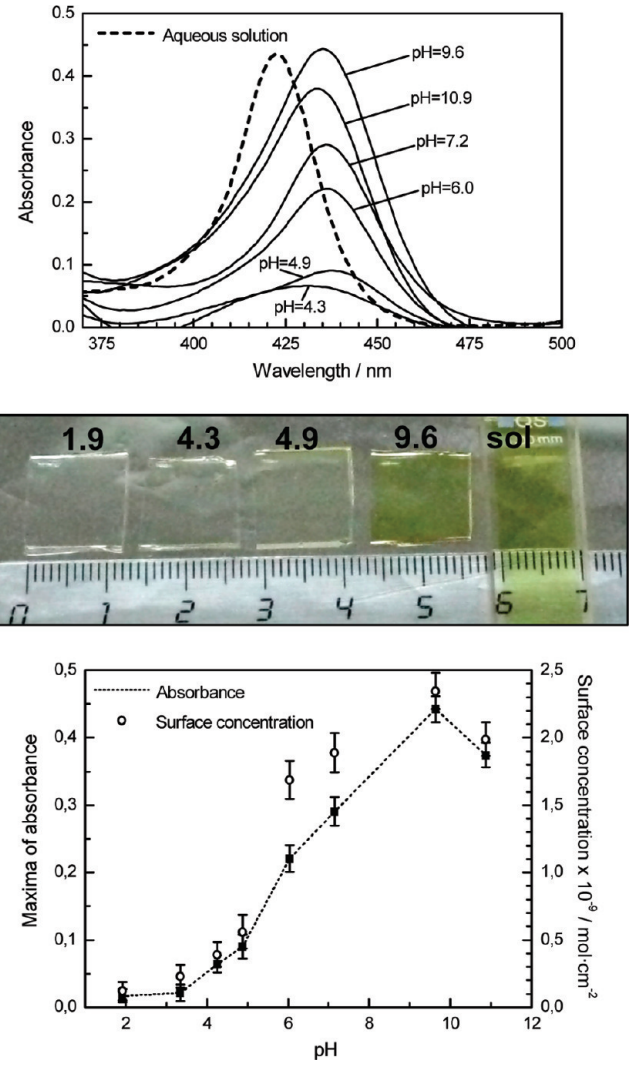

FIGURE 5. (Top) Absorption spectra for a series of composite TMPyP/TiO_2 thin films prepared by infiltration from aqueous solutions at different pHs as indicated. The figure shows the Soret Band. (Bottom) Evolution of the absorption intensity of the spectra and the amount of molecules infiltrated into the film as a function of the pH during the infiltration procedure. (Middle) Images taken for actual films prepared at the indicated pHs and a 4×10^{-5} M water solution.

the point of zero charge (PZC) theory of colloids, immersion of an oxide at a pH higher than its PZC leads to the development of a negative charge on its surface by dissociation of the −OH surface groups. This charge is compensated by cations in the double layer of charge.

The fact that a significant infiltration of TMPyP molecules into the TiO_2 thin films only occurs for pHs equal or higher than 5.5 (i.e., close to its point of zero charge, PZC) (36, 37) indicates that incorporation the of dye molecules into the pores of the thin films is favored when there is an excess of negative charge distributed onto its internal surface. Such electrostatic interaction has been also claimed for other related composite systems (38). As the pH increases, the amount of negative charges on the TiO_2 surface increases, and subsequently the amount of required positive charges (dye molecules) to compensate this negative charge invariably grows. Incorporation stops at a pH of about 11, where the amount of adsorbed TMPyP molecules slightly de-

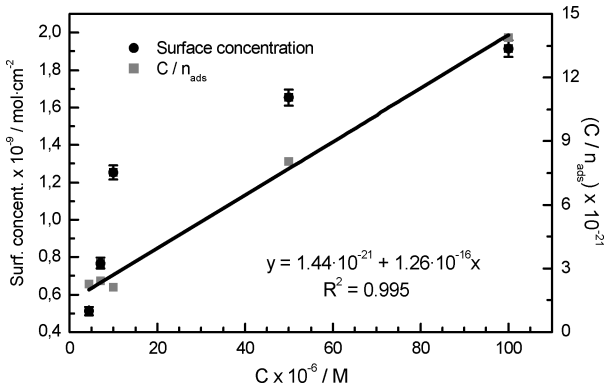

FIGURE 6. Langmuir adsorption plots for a TMPyP infiltration into TiO_2 thin films.

creases. The observed pH dependence confirms the electrostatic nature of the TMPyP/TiO_2 interaction in the composite films.

Adsorption Equilibrium. Besides pH, another important factor affecting the infiltration capacity of the columnar films is the concentration of the dye in the original solution. Different samples have been prepared by changing this parameter during the preparation. Figure 6 depicts, for pH 6.0 and a 1 h of infiltration time, the surface concentration (Γ) of the dye in the different films for increasing concentrations in the water solutions used for the infiltration. It is clear that the amount of incorporated porphyrin molecules increases when increasing the solution concentration. For small concentrations, the infiltration capacity is already high and sharply increases to reach a high value at a solution concentration of around 1×10^{-5} M. For more concentrated solutions, the film starts to become saturated. A similar behavior was found for other pHs in the range comprised between 5 and 10, with the saturation value following a tendency similar to that in Figure 5 corresponding to a dye concentration of 1×10^{-5} M.

A better picture for the concentration dependence of the infiltration process can be obtained by applying an isotherm model to the data points in Figure 6 (39). The Langmuir adsorption isotherm (40) has been successfully used to account for the adsorption of different types of molecules either from gas or liquid media onto different solid materials (41−43). The Langmuir adsorption isotherm can be expressed by

$$\frac{n_{ads}}{N_S} = \frac{\lambda c}{1 + \lambda c} \qquad (3)$$

Where n_{ads} is the number of the adsorbed molecules, N_S is the number of adsorption sites available on the TiO_2 surface, λ is a constant relating to the adsorption capacity of TMPyP, and c is the concentration of the dye in solution.

Rearrangement of eq 3 leads to the linear form of the Langmuir adsorption isotherm, where a plot of c/n_{ads} versus c should yield a straight line if the data points actually follow the Langmuir model. This plot has been added in Figure 6 and shows the actual number of adsorbed porphyrin molecules (n_{ads}) as a function of the dye concentration in solution. The straight line obtained indicates that a Langmuir adsorption provides a good description of the TMPyP/TiO_2 interaction during the infiltration process. According to the basic assumptions of the Langmuir model, one can conclude the following features as characteristics of the adsorption and infiltration process: (i) the adsorption energy of all TMPyP molecules incorporated into the film is quite similar; (ii) there is a limited number of adsorption sites at a given pH; (iii) one of these sites, once occupied by a molecule, cannot contribute to an additional incorporation of TMPyP.

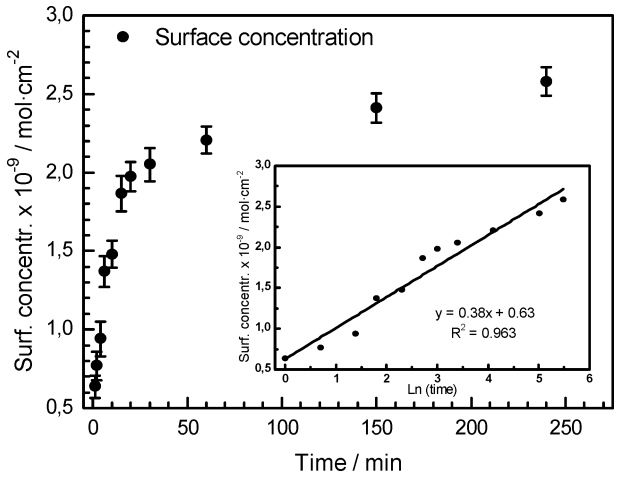

FIGURE 7. Kinetic adsorption experiments obtained by desorption. All the experiments were carried out at least four times.

Adsorption Kinetics. The infiltration of the TMPyP molecules into the columnar TiO_2 films is a time dependent process. Figure 7 shows the time evolution of the porphyrin surface concentration Γ as it becomes incorporated into a 350 nm thick TiO_2 film at a pH of the solution of 6.9 and a solution concentration of 1×10^{-5} M. The curve defined by the different data points can be divided in two parts, a first one characterized by a fast growth of the amount of infiltrated molecules followed by a much slower process where the film is approaching saturation.

To further characterize the infiltration process, we have tried to adjust the experimental points in Figure 7 with different kinetic models of adsorption. It was found that an Elovich kinetic model (44) fitted well the experimental points (45). According to the integrated form of the Elovich equation, typically used in chemisorption studies, the evolution of the surface coverage Θ as a function of time, t, is given by

$$\Theta = \left(\frac{1}{\beta}\right)\ln(t) + K \qquad (4)$$

where β and K are constants. Equation 4 indicates that there is an exponential decrease of the rate of the surface adsorption as the coverage of the surface increases. Using Γ as an equivalent magnitude to Θ, we have found a good fitting to the model as reported in the inset of Figure 7, where the points define an almost linear relationship over the entire range of times studied. This indicates that the probability of

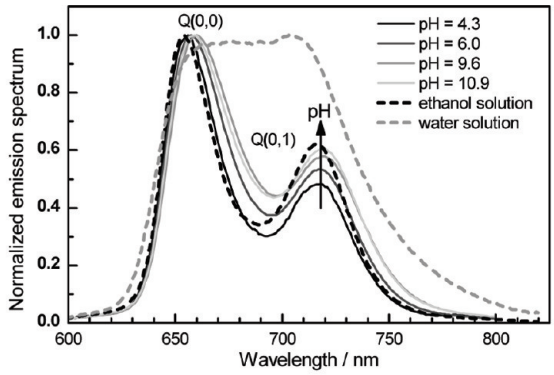

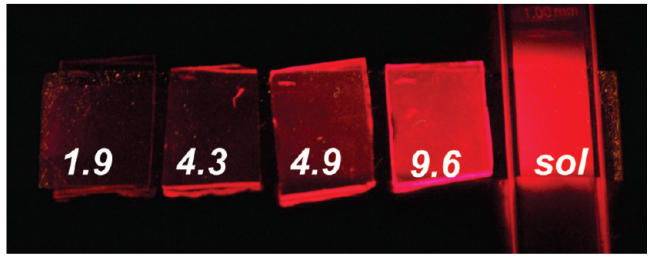

FIGURE 8. (Top) Normalized fluorescence spectra recorded for the samples whose absorption spectra is represented in Figure 4. (Bottom) Images taken for actual films prepared at the indicated pHs and a 4×10^{-5} M water solution that are being illuminated with a low energy fluorescent lamp, 4 W, 365 nm.

adsorption of a TMPyP molecule decreases exponentially with the number of occupied adsorption sites (or adsorbed TMPyP molecules) on the surface of the columnar TiO_2 structure. Moreover, the good fitting with the Elovich equation reveals that the TiO_2 columnar microstructure not only exhibits a very good infiltration capacity but also an excellent accessibility of the incoming porphyrin molecules to the active adsorption sites.

Fluorescence Behavior of TMPyP/TiO_2 Composite Films. Figure 8 shows a representation of the normalized fluorescence spectra recorded for the films whose absorption spectra as a function of the pH are reported in Figure 5. Spectra of ethanol and aqueous TMPyP 1×10^{-5} M solutions have been included for comparison. The ethanol solution presents two well-differentiated bands corresponding to the degeneracy of the lowest singlet configuration of the TMPyP (46). These two bands, Q(0,0) and Q(0,1), are centered approximately at 654 and 716 nm. In the water solution, the bands appear at 666 and 704 nm and are less resolved than in ethanol. This difference has been attributed to a change in the resonance interaction between the pyridinium group and the π system of the porphyrin macrocycle because of the polarity of the media (47). For aqueous solutions, this resonance interaction increases and results in an overlapping between the two bands (27, 47).

The shape of the spectra in Figure 8 of the TMPyP/TiO_2 films as a function of the infiltration pH differs from that of the aqueous solution and is similar to that of the ethanol solution. This supports a significant change in the conformation of the molecule with respect to the aqueous solution, very likely because of its interaction with the TiO_2 surface. A closer look to these spectra reveals that the Q(0,0) band gradually shifts from 655 nm at a pH 4.3 to 660 nm at a pH

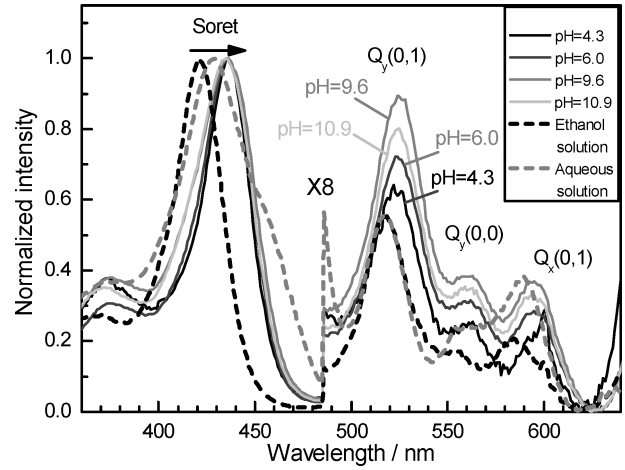

FIGURE 9. Normalized excitation spectra recorded for the samples whose absorption spectra are represented in Figure 5. The excitation spectra of a 1×10^{-5} M ethanol and water solution have been added for comparison.

10.9, whereas the Q(0,1) band appears fixed at 719 nm for all the pHs. It is also visible that the intensity ratio of these two bands changes progressively with the infiltration pH from a value of 0.48 (pH 4.3) to 0.61 (pH 10.9). Spectral changes depicting similar tendencies can be evidenced when comparing the spectra of TMPyP in aqueous solutions or in solid media (47, 48). These spectral changes, usually more pronounced in liquid solutions than in solids, have been related with changes in the conformation of the molecule and found to be very much dependent on the dielectric constant of the surrounding medium (47). The fact that in our films the magnitude of the changes with the pH is relatively small suggests that the conformational changes with the pH are not very pronounced and that the TMPyP molecules, although anchored onto the surface of TiO_2, are not totally surrounded by this high dielectric constant material.

For illustration, Figure 8 (bottom) shows a photograph of the same samples than in the picture included in Figure 5, but illuminated with a low energy fluorescent lamp of 365 nm. It is apparent that the fluorescence of the different samples increases toward the sample prepared at pH 9.6 and that the fluorescence of this composite thin film is comparable with that of the water solution.

Figure 9 shows the normalized excitation spectra of the composite films as a function of the infiltration pH and those of aqueous and ethanol solutions included for comparison. It must be mentioned that the spectra of the films, even for low loaded samples, correspond directly to the excitation bands of the molecule discarding any possible contribution due to the interference oscillations of the TiO_2 substrate (see experimental section and the Supporting Information, Figure S1). These excitation spectra, very similar in shape to the UV−vis spectra reported in Figure 5, are characterized by an intense Soret band at around 425 nm and the set of Q bands in the spectral range between 500 and 625 nm. Both the Soret and Q bands of the composite thin films are red-shifted with respect to these bands in the two liquid solutions used for comparison. According to the literature, the red shift

in the wavelengths of the bands can be attributed to a flattening of the molecule (i.e., a twist in the angle of the pyridinium methyl group (29, 49),) and/or to some J-aggregation (28).

Another interesting observation in the previous spectra is the appearance of a weak band at longer wavelengths (λ > 625 nm) not reported in the figure, ($Q_x(0,0)$). It is also worth noting that a comparison between the excitation and absorption spectra for the difference pHs (see such a comparison for pH 6.0 and 9.6 in the Supporting Information, Figure S4) reveals a quite good correspondence in spectral shapes. This similarity supports the absence of H dimers that might absorb light without subsequent fluorescence emission and that the excitation bands can be used for a more accurate determination of the wavelengths of the maxima. Thus, it can be established that the Soret band slightly changes from 437 to 435 nm when the pH increases from 4.3 to 9.6. Additionally, a continuous broadening of the band is apparent as the pH increases. Meanwhile, no significant change is observed in the wavelengths of the Q bands. This contrasts with the fact that their intensities increase with the infiltration pH, reaching a maximum at pH 9.6 and then decreasing for a pH of 10.9. Q bands are very sensitive to changes in the conformational structure of the molecules. In our case the increase in the Q-band intensity with the pH confirms a progressive change in the adsorption state of the molecules with this parameter (48).

Exposure of the TMPyP/TiO_2 Composite Films to HCl Vapors. The potential use of the TMPyP/TiO_2 composite film for gas sensing applications rely on two necessary (although not sufficient) conditions: (i) the modification of the optical response of the dye molecules by their interaction with gases and (ii) the accessibility of these gases to the sensing molecules even if they are trapped into the pores of the TiO_2 films. The reversibility of the interaction process is another related condition for this purpose. To address these points with our films, we have carried out a very simple experiment consisting of the exposure of the TMPyP/TiO_2 composite thin films to the vapors of a concentrated HCl solution at 37%. The ability of the TMPyP molecule to protonate in acid solutions is a well-known property of this molecule (the pK of the TMPyP is arround 1,5) (27) that has been proposed as pH sensor when deposited onto a glass plate (35). The results of our experiment are shown in Figure 10, where the changes in the UV−vis absorbance (top) and the fluorescence spectra (bottom) are reported. In Figure 10 (top), it is observed that exposure of the films for less than one second to acid vapors drastically changes the shape of the whole absorption spectrum. The fact that practically no contribution of the original band remains in the spectrum supports that virtually all the TMPyP molecules have been affected by the acid exposure. To a first approximation, the spectral changes can be characterized by a shift of the Soret band by 25 nm and a drastic decrease in the intensity of the fluorescence spectrum. A quite similar shift in the Soret band has been reported by Kalimuthu et al. (50) in the above-mentioned work where these authors

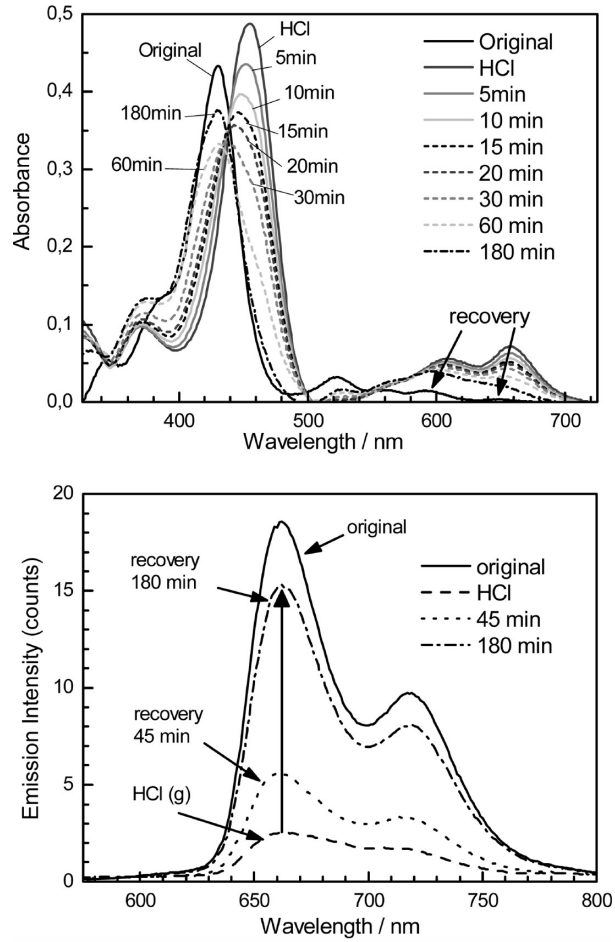

FIGURE 10. Absorption (top) and fluorescence (bottom) spectra of the change and recovery under HCl exposure.

attributed this effect to the protonation of the molecule. Protonation is further supported in our case by the drastic decrease in the intensity of the two first Q_y bands at 522 and 560 nm and the enhancement of the intensity of the Q_x bands at 592 and 648 nm because of a loss of the D_{2h} symmetry of the molecule (27, 30). As shown in Figure 10 (bottom), the protonation of the TMPyP molecule produces a drastic decrease in the fluorescence intensity. Similar results has been obtained by Kalimuthu et al. (50).

The possible use of the dye/TiO_2 composite thin films as optical sensors is further sustained by the fact that, according to Figure 10, the absorption and the fluorescence spectra almost recover their initial intensity and shape by leaving the sample in air for 3 h. This recovery of the shape of the spectra indicates that the process is reversible and therefore the infiltrated molecules can undergo an exchange process with the environment. Looking at the possibility of using our films as real photonic sensors, preliminary experiments with the sample at t > 50 °C have shown that this recovery process is drastically accelerated. Further work is being carried out at present in our group to ascertain this behavior and develop real sensor materials based on optically active porphyrin/TiO_2 composite films.

CONCLUSIONS

In this work, we have investigated the infiltration process of TMPyP molecules within very porous but optically transparent TiO_2 thin films prepared by GAPVD. The total porosity of these films and their pore size distribution has been assessed by measuring water adsorption isotherms. Because the prepared composite films did not disperse the light, they are deemed appropriate for their implementation in optical and photonic devices. In comparison with polymers and other similar matrixes, where processes like deformation and swelling may occur on exposure to certain analytes, advantages of our films are their robustness and the fact that their initial state can be recovered by pumping and/or heating at moderate temperatures.

The incorporation process of the porphyrin dye, consisting of the infiltration of the dye molecules from an aqueous solution, was highly dependent on the pH and can be explained by using the PZC concepts used to account for the evolution of the surface charge on oxide suspensions. The incorporation process can be described according to the Langmuir adsorption model, whereas the kinetics of incorporation follows an Elovich equation. This description of the equilibrium and kinetics of the adsorption discards that diffusion plays a significant role in limiting the accessibility of the TMPyP molecules to the voids of the thin film, and that the number of adsorption sites is the controlling factor of the infiltration process at each pH.

The optical properties of the composite TMPyP/TiO_2 thin films have been investigated by absorption and fluorescence spectroscopies. Although the actual state of the molecules within the films has not been unraveled yet, the assessment of these spectra confirm a tight interaction of the molecule, very likely in the form of monomer, with the surface of the TiO_2, although the formation of J-dimers cannot be excluded. The easy accessibility of gases to all dye molecules and the reversibility of the process in a preliminary experiment consisting of the exposure of the composite films to acid vapors suggests that these types of optically active thin films are potentially good materials to develop into optical gas sensors.

Acknowledgment. We thank the Ministry of Science and Education of Spain (Projects MAT 2007-65764/NAN2004-09317 and PET2007_0363_01/_02), the Regional Government of Andalusia (Project P07-FQM-03298), and Sos Cuétara S.A. for financial support.

Supporting Information Available: Measured and simulated UV−vis transmission spectra for TiO_2 thin films on glass for refractive index determination (Figure S1); method for the determination of the TMPyP surface concentration directly from the spectra of the films (Figure S2); UV−vis absorbance spectra for TMPyP/TiO_2 composites using unpolarized and s- and p-polarized light, for an angle of incidence of 45° (Figure S3); normalized fluorescence excitation and absorbance spectra for the composites infiltrated at different pHs (Figure S4) (PDF). This material is available free of charge via the Internet at http://pubs.acs.org.

REFERENCES AND NOTES

(1) Kay, A.; Grätzel, M. *J. Phys. Chem.* **1993**, *97*, 6272.
(2) O'Regan, B.; Grätzel, M. *Nature* **1991**, *334*, 737.
(3) Whitlock, J. B.; Panayotatos, P.; Sharma, G. D.; Cox, M. D.; Sauers, R. R.; Bird, G. R. *Opt. Eng.* **1993**, *32*, 1921.
(4) Huijser, A.; Savenije, T. J.; Meskers, S. C. J.; Vermeulen, M. J. W.; Siebbeles, L. D. A. *J. Am. Chem. Soc.* **2008**, *130*, 12496.
(5) Gupta, T.; Van der Boom, M. E. *J. Am. Chem. Soc.* **2006**, *128*, 8400.
(6) Rakow, N. A.; Suslick, K. S. *Nature* **2000**, *406*, 710.
(7) (a) Vergeldt, F. J.; Koehorst, R. B. M.; Schaafsma, T. J.; Lambry, J. C.; Martin, J. L.; Johnson, D. G.; Wasielewski, M. R. *Chem. Phys. Lett.* **1991**, *182*, 107. (b) Neumann-Spallart, M.; Kalyanasundaram, K. *J. Phys. Chem.* **1982**, *86*, 5163.
(8) (a) Prieto, I.; Pedrosa, J. M.; Martín-Romero, M. T.; Möbius, D.; Camacho, L. *J. Phys. Chem. B* **2000**, *104*, 9966. (b) Mareé, C. H. M.; Savenije, T. J.; Schaafsma, T. J.; Habraken, F. H. P. M. *Appl. Surf. Sci.* **1996**, *93*, 291.
(9) (a) Gaillon, L.; Bedioui, F.; Devynck, J.; Battioni, P. *J. Electroanal. Chem.* **1993**, *347*, 435. (b) Bettelheim, A.; Ozer, D.; Harth, R.; Murray, R. W. *J. Electroanal. Chem.* **1989**, *266*, 93.
(10) Harriman, A.; Heitz, V.; Ebersole, M.; Vanwilligen, H. *J. Phys. Chem.* **1994**, *98*, 4982.
(11) (a) Gulino, A.; Giuffrida, S.; Mineo, P.; Purrazzo, M.; Scamporrino, E.; Ventimiglia, G.; Van Der Boom, M. E.; Fragalà, I. *J. Phys. Chem. B* **2006**, *110*, 16781. (b) Yerushalmi, R.; Scherz, A.; Van Der Boom, M. E. *J. Am. Chem. Soc.* **2004**, *126*, 2700.
(12) Sánchez-Valencia, J. R.; Borrás, A.; Barranco, A.; Rico, V. J.; Espinós, J. P.; González-Elipe, A. R. *Langmuir* **2008**, *24*, 9460.
(13) Sanchez-Valencia, J. R.; Blaszczyk-Lezak, I.; Espinos, J. P.; Hamad, S.; Gonzalez-Elipe, A. R.; Barranco, A. *Langmuir* **2009**, *25*, 9140.
(14) Holze, R. *Electrochim. Acta* **1988**, *33*, 1619.
(15) Khanova, L. A.; Lafi, L. F. *J. Electroanal. Chem.* **1993**, *345*, 393.
(16) Itoh, K.; Sugii, T.; Kim, M. *J. Phys. Chem.* **1988**, *92*, 1569.
(17) Fierro, C. A.; Mohan, M.; Scherson, D. A. *Langmuir* **1990**, *6*, 1338.
(18) Kim, S.; Bae, L. T.; Sandifer, M.; Ross, P. N.; Carr, R.; Woicik, J.; Antonio, M. R.; Scherson, D. A. *J. Am. Chem. Soc.* **1991**, *113*, 9063.
(19) Brett, M. J.; Hawkeye, M. M. *Science* **2008**, *319*, 1192.
(20) Hawkeye, M. M.; Brett, M. J. *J. Vac. Sci. Technol., A* **2007**, *25*, 1317.
(21) Robbie, K.; Brett, M. J. *J. Vac. Sci. Technol., A* **1997**, *15*, 1460.
(22) Wang, S.; Xia, G.; He, H.; Yi, K.; Shao, J.; Fan, Z. *J. Alloys Compd.* **2007**, *431*, 287.
(23) Kiema, G.; Colgan, M. J.; Brett, M. J. *Sol. Energy Mater. Sol. Cells* **2005**, *85*, 321.
(24) Borrás, A.; Sánchez-Valencia, J. R.; Garrido-Molinero, J.; Barranco, A.; González-Elipe, A. R. *Microporous Mesoporous Mater.* **2009**, *118*, 314.
(25) (a) Borrás, A.; Cotrino, J.; González-Elipe, A. R. *J. Electrochem. Soc.* **2007**, *154*, 152. (b) Borrás, A.; Barranco, A.; González-Elipe, A. R. *J. Mater. Sci.* **2006**, *41*, 5220.
(26) (a) Broughton, J. N.; Brett, M. J. *Electrochem. Solid-State Lett.* **2002**, *5*, A279. (b) Harris, K. D.; Brett, M. J.; Smy, T. J.; Backhouse, C. *J. Electrochem. Soc.* **2000**, *147*, 2002.
(27) Kalyanasundaram, K. *Inorg. Chem.* **1984**, *23*, 2453.
(28) de Miguel, G.; Pérez-Moales, M.; Martín-Romero, M. T.; Muñoz, E.; Richardson, T. H.; Camacho, L. *Langmuir* **2007**, *23*, 3794.
(29) Chernia, Z.; Gill, D. *Langmuir* **1999**, *15*, 1625–1633.
(30) Dixon, D. W.; Pu, G.; Wojtowicz, H. *J. Chromatogr. A* **1998**, *802*, 367.
(31) Xi, J.-Q.; Kim, J. K.; Schubert, E. F. *Nano Lett.* **2005**, *5*, 1385.
(32) *Adsorption, Surface Area and Porosity*; Gregg, S. J., Sing, K. S. W., Eds.; Academic Press: London, 1982.
(33) Dargiewicz, J.; Makarska, M.; Radzki, S. *Colloid Surf., A* **2002**, *208*, 159.
(34) Siskova, K.; Vlckova, B.; Mojzes, P. *J. Mol. Struct.* **2005**, *744*, 265.
(35) Itagaki, Y.; Deki, K.; Nakashima, S.-I.; Sadaoka, Y. *Sens. Actuators, B* **2006**, *117*, 302.
(36) *Chemical Properties of Material Surfaces*; Kosmulski, M., Ed.; Marcel Dekker: New York, 2001.
(37) *Principles of Colloids and Surface Chemistry*; Hiemenz, P. C., Rajagopalan, R., Eds.; Marcel Dekker: New York, 1997.
(38) Savenije, T. J.; Marée, C. H. M.; Habraken, F. H. P. M.; Koehorst, R. B. M.; Schaafsma, T. J. *Thin Solid Films* **1995**, *265*, 84.
(39) Altin, O.; Ozbelge, O.; Dogu, T. *J. Colloid Interface Sci.* **1998**, *1*, 130.

(40) Langmuir, I. *J. Am. Chem. Soc.* **1918**, *40*, 1361.
(41) Worsfold, O.; Dooling, C. M.; Richardson, T. H.; Vysotsky, M. O. *J. Mater. Chem.* **2001**, *11*, 399.
(42) Changue, B.; Germain, J. P.; Maleysson, C.; Robert, H. *Sens. Actuators* **1985**, *7*, 199.
(43) Goldberg, S. *Plant Soil* **1997**, *193*, 35.
(44) Elovich, S. Y.; Zhabrova, G. M. *J. Phys. Chem.* **1939**, *13*, 1761.
(45) Cabrejas, M.; Guil, J. M.; Ruiz, A. *J. Chem. Soc., Faraday Trans.* **1 1989**, *85*, 1775.
(46) Spellane, P. J.; Gouterman, M.; Antipas, A.; Kim, S.; Liu, Y. C. *Inorg. Chem.* **1980**, *19*, 386.
(47) Vergeldt, F. J.; Koehorst, R. B. M.; van Hoek, A.; Schaafsma, T. J. *J. Phys. Chem.* **1995**, *99*, 4397.
(48) Ou, Z.-M. *J. Photochem. Photobiol., A* **2007**, *189*, 7.
(49) Luca, G. D.; Romeo, A.; Scolaro, L. M. *J. Phys. Chem. B* **2005**, *109*, 7149.
(50) Kalimuthu, P.; Abraham, J. S. *Anal. Chim. Acta* **2008**, *627*, 247.

AM900746Q